

A TRIPLE WIRE MEDIUM AS AN ISOTROPIC NEGATIVE PERMITTIVITY METAMATERIAL

M. Hudlička and J. Macháček

Department of Electromagnetic Field
Faculty of Electrical Engineering
Czech Technical University in Prague
Technická 2, 16627 Prague 6, Czech Republic

I. S. Nefedov

Institute of Radio Engineering and Electronics
Russian Academy of Sciences
410019 Zelyonaya 38, Saratov, Russia

Abstract—This paper presents an effective medium approach to calculate the attenuation and phase constants of modes in a 3D connected wire medium both below and above the plasma frequency. Physical and nonphysical modes in the structure are identified for all the important lattice directions. According to this, the medium behaves as an isotropic material in the vicinity of the plasma frequency. These results were compared with the numerical simulation and it was observed that the wave spreads below the plasma frequency along all the important lattice directions with the same attenuation constant. This implies isotropic behavior of the 3D wire lattice below the plasma frequency, and thus this medium can be considered as an isotropic negative permittivity medium.

1. INTRODUCTION

The medium formed by a two-dimensional lattice of ideally conducting parallel thin wires (wire medium) has been known for a long time [1–5]. When the wavelength of the incident radiation is much longer than the intrinsic length-scales of the structure, it is very helpful to consider this medium as a homogeneous material with averaged constitutive material parameters (effective medium theory). In the framework of effective medium (EM) theory, wire media (WM) are described by the

plasma model, where the corresponding component of the permittivity dyadic is expressed by the Drude formula. Pendry et al. [6, 7] and Sievenpiper [8] have independently demonstrated that metallic wire-mesh structures have a low frequency stop band from zero frequency to the cutoff frequency. They attributed this to the motion of the electrons in the metal wires. This low frequency stop band can be attributed to effective negative dielectric permittivity, and, when the wire lattice dimensions are chosen properly, negative permittivity can be obtained even at microwave frequencies [6]. Recently the plasma model has been corrected by introducing spatial dispersion (SD) into the Drude formula [9]. Spatial dispersion can be defined as a nonlocal dispersive behavior of the material, i.e., the constitutive permittivity and permeability tensors depend not only on the frequency, but also on the spatial derivatives of the electric and magnetic field vectors or, for plane electromagnetic waves, on the wave-vector components determining the direction of propagation. Initially, a strong spatial dispersion effect was predicted only in the short-wavelength limit [9]. In recent years, modes in both connected and nonconnected double wire media have been studied [10–13] and spatial dispersion effects have been discussed not only at low frequencies, but even above plasma resonant frequencies. Recently a general vector circuit representation for the description of spatially dispersive uniaxial magneto-dielectric slabs was presented in [14]. The developed method can also be applied to study the transmission characteristics of the slab only in the presence of wires.

Silveirinha and Fernandes [10] described the behavior of both connected and nonconnected *triple* wire lattices. In this paper, a permittivity tensor was derived, which corresponds to a sophisticated plasma model describing the wire mesh [15]. For the construction of an isotropic negative permittivity material, a triple connected wire mesh system seems to be promising [10], as it exhibits weak spatial dispersion. A simple model of cold plasma was used by Shapiro et al. [16], who observed the surface waves at the interface between the wire mesh and the free space, and studied the influence of spatial dispersion on these waves.

The analysis of the medium consisting of the 3D mesh of connected wires presented here uses the effective medium approach proposed in [10]. Assuming propagation of a plane wave, Maxwell equations with the applied tensor of an effective permittivity, derived in [10], give an eigenvalue system of equations for possible eigen modes propagating in the medium. The resulting dispersion equation takes into account the spatial dispersion. The geometry of the unit cell is depicted in Fig. 1. The wire mesh has a period a , and the wires have radius r_w .

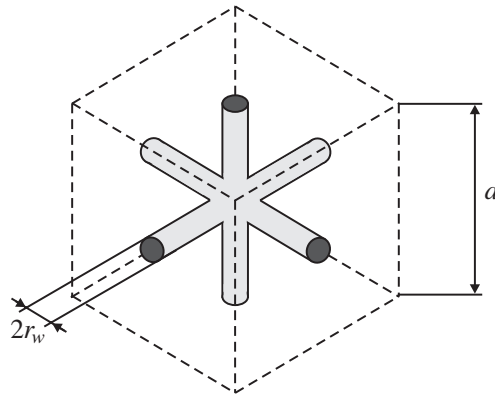


Figure 1. Triple wire mesh structure formed by a lattice of infinitely long connected wires.

The structure is assumed to be lossless.

The dispersion characteristics are shown for particular specific directions of the first Brillouin zone together with the characteristics determined by the commercial full-wave simulator CST Microwave Studio (MWS) [17]. An original numerical experiment is proposed to verify the theory. The triple wire medium is modeled by MWS as a sphere filled with a system of mutually perpendicular connected wires. This system is excited by a dipole located at the center of the sphere. The electric field distribution is calculated. This field is naturally perturbed by the wires, and is not averaged as the field used to determine the effective permittivity tensor [10]. Nevertheless, it can be compared with the field radiated into an empty space, except for attenuation due to the negative permittivity. This simulates the omnidirectional propagation of a wave in the triple WM both below and above the plasma frequency. The results confirm the suitability of the triple wire medium to be applied as an isotropic negative permittivity metamaterial near the plasma frequency.

2. EFFECTIVE PERMITTIVITY DYADIC, DISPERSION EQUATION

In this work we adopt the relative effective permittivity dyadic describing the homogenized medium of 3D connected wires obtained in [10]. This effective permittivity dyadic corresponds to the permittivity of a nonmagnetized plasma, where the pressure forces are considered

[15], and reads

$$\bar{\bar{\epsilon}} = \bar{\mathbf{I}} - \frac{k_p^2}{k_0^2} \left(\bar{\mathbf{I}} - \frac{\mathbf{k}\mathbf{k}}{k^2 - l_0 k_0^2} \right), \quad (1)$$

where k_p is the plasma wave number, k_0 is the free-space wave number, and

$$l_0 = \frac{3}{1 + 2k_p^2/\beta_1^2}, \quad (2)$$

$$\frac{1}{\beta_1^2} = \left(\frac{a}{2\pi} \right)^2 \sum_{l \neq 0} \frac{[J_0(\frac{2\pi l r_w}{a})]}{l^2}, \quad (3)$$

where a is the lattice period, r_w is the wire radius and J_0 stands for the Bessel function of the first kind and order zero. In [18] there are two formulas for the plasma wave number of such a wire array

$$(k_p a)^2 \approx \frac{2\pi}{\ln\left(\frac{a}{2\pi r_w}\right) + 0.5275} \quad (r_w < a/100), \quad (4)$$

$$(k_p a)^2 \approx \frac{2\pi}{\ln\left(\frac{a^2}{4r_w(a-r_w)}\right)} \quad (a/20 < r_w < a/5). \quad (5)$$

The effective permittivity dyadic depends explicitly on the wave vector, and thus the medium suffers in general from spatial dispersion. The dispersion equation can be derived from Maxwell's equations of the form

$$\nabla \times \mathbf{E} = -j\omega\mu_0\mathbf{H}, \quad (6)$$

$$\nabla \times \mathbf{H} = j\omega\epsilon_0\bar{\bar{\epsilon}}\mathbf{E}, \quad (7)$$

where the electric and magnetic field intensity are expected to be in the form of plane waves

$$\mathbf{E}(\mathbf{r}) = \mathbf{E}_0 \exp[-j(\mathbf{k} \cdot \mathbf{r})] = \mathbf{E}_0 \exp[-j(k_x x + k_y y + k_z z)], \quad (8)$$

$$\mathbf{H}(\mathbf{r}) = \mathbf{H}_0 \exp[-j(\mathbf{k} \cdot \mathbf{r})] = \mathbf{H}_0 \exp[-j(k_x x + k_y y + k_z z)]. \quad (9)$$

By solving the set of Equations (6), (7) and assuming $k_0^2 = \omega^2\epsilon_0\mu_0$ and $k^2 = k_x^2 + k_y^2 + k_z^2$ and the electromagnetic field in the form (8) and (9), we come to the eigenvalue equation

$$\begin{pmatrix} k_0^2\epsilon_{xx} - k_z^2 - k_y^2 & k_x k_y + k_0^2\epsilon_{xy} & k_x k_z + k_0^2\epsilon_{xz} \\ k_x k_y + k_0^2\epsilon_{yx} & k_0^2\epsilon_{yy} - k_x^2 - k_z^2 & k_y k_z + k_0^2\epsilon_{yz} \\ k_x k_z + k_0^2\epsilon_{zx} & k_y k_z + k_0^2\epsilon_{zy} & k_0^2\epsilon_{zz} - k_y^2 - k_x^2 \end{pmatrix} \begin{pmatrix} E_x \\ E_y \\ E_z \end{pmatrix} = 0. \quad (10)$$

Solving (10) means finding the eigen values k_x , k_y , k_z for eigen waves E_x , E_y , E_z . Rewriting the determinant of (10) into dyadic form we obtain the dispersion equation as in [10]

$$\det(\mathbf{k}\mathbf{k} - k^2\bar{\mathbf{I}} + k_0^2\bar{\bar{\epsilon}}) = 0. \quad (11)$$

The dispersion characteristics of the particular modes are determined by solving this dispersion equation.

3. DISPERSION CHARACTERISTICS

Throughout the text we adopt $a = 10$ mm, $r_w = 0.5$ mm, and thus the plasma wave number is $k_p = 194.509 \text{ m}^{-1}$, $\beta_1 = 394.303 \text{ m}^{-1}$ and the constant $l_0 = 2.018$. The corresponding plasma frequency calculated using (5) is approx. $f_p = 9.28$ GHz. First, we assume the case of $k_z = 0$ and $k_x \neq k_y$, thus we can obtain isofrequencies k_x as a function of k_y for the wave propagating in the x - y plane. In this simplified case, the determinant in (10) has the form of a polynomial of the variable k_y of the sixth order, and thus generally has 6 roots, which correspond to 3 eigen waves, i.e., 3 sets of solutions with positive and negative sign. The dependence of k_y on k_x can be expressed for the first solution as follows

$$k_{y1}^2 = k_0^2 - k_x^2 - k_p^2, \quad (12)$$

whereas the other solutions are nonphysical and they read

$$k_{y2}^2 = \frac{1}{2k_0^2} (K_1 - K_2), \quad (13)$$

$$k_{y3}^2 = \frac{1}{2k_0^2} (K_1 + K_2), \quad (14)$$

where

$$K_1 = k_0^4 (l_0 + 1) + 4k_x^2 k_p^2 - k_0^2 [2k_x^2 + k_p^2 (l_0 + 1)], \quad (15)$$

$$K_2 = \sqrt{k_0^2 - k_p^2} \sqrt{(k_0^6 - 16k_p^2 k_x^4 - k_0^4 k_p^2)(l_0 - 1)^2 + 8k_0^2 k_p^2 k_x^2 (l_0 + 1)}. \quad (16)$$

Equation (12) corresponds to Equation (7) in [9], setting $k_z = 0$. The propagation constant (12) is shown in Fig. 2 for two different ratios k_0/k_p . The plots in Figs. 2(a) and 2(b) represent circles, which means that the corresponding wave propagates in the x - y plane with the same propagation constant in all directions. The frequency dependence of the propagation constant modulus from (12) is shown in Fig. 3 both

below and above the plasma frequency f_p . The curve below the plasma frequency corresponds to the case when both k_x and k_y are pure imaginary. Thus the size of k represents the size of the attenuation constant. In the case above the plasma frequency, k_x and k_y are considered to be real and the size of k represents the size of the phase constant. The point where both the real and the imaginary parts drop to zero corresponds to the plasma frequency f_p . By changing the frequency, we only change the size of k . This is a verification of the results obtained in Fig. 2, since the dependence of k_y on k_x is always a circle for any frequency (except of f_p , where $k = 0$).

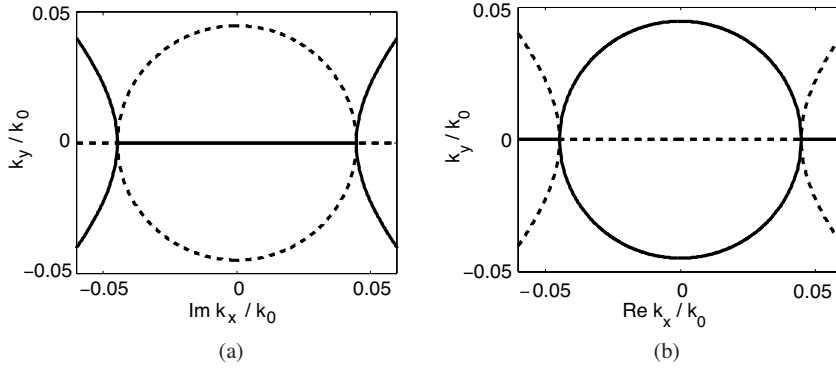


Figure 2. Dependence $k_{y1} = f(k_x)$ (12) for the ratio $k_0/k_p = 0.999$ below the plasma frequency (a), and $k_0/k_p = 1.001$ above the plasma frequency (b). The solid line corresponds to the real part, and the dashed line corresponds to the imaginary part of the propagation constant k_{y1} .

The other specific case is $k_i \neq 0$ ($i = x, y, z$) and the other two components are equal to zero, thus we observe only the wave propagation along one axis. This corresponds to the Γ - X direction in the first Brillouin zone. The frequency dependence of component k_i now reads

$$k_{i1}^2 = k_{i2}^2 = k_0^2 - k_p^2 \quad i = x, y, z, \quad (17)$$

$$k_{i3}^2 = (k_0^2 - k_p^2) l_0 \quad i = x, y, z. \quad (18)$$

It is obvious that (17) is a simplification of (12), and the plot in Fig. 3 can be adopted for it, changing $\sqrt{k_x^2 + k_y^2}$ on its vertical axis to just k_i , since the propagation of the wave along one axis is equivalent to the propagation along the unit cell face, i.e., in the x - y

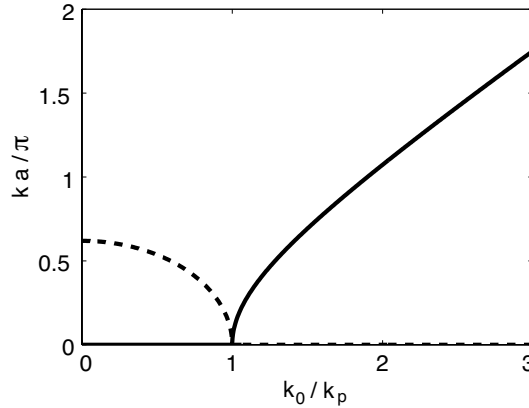


Figure 3. Frequency dependence of the size of the propagation constant $k = \sqrt{k_x^2 + k_y^2}$ both below (dashed line, imaginary part) and above (solid line, real part) the plasma frequency, for the case $k_z = 0$ and $k_x \neq k_y \neq 0$.

plane. Solution (17) was identified as a TEM mode and solution (18) as a longitudinal mode in [10]. Solution (18) is identical with (17), except for the value of the propagation constant, and has the same frequency dependence. The case of $k_x = k_y$ and $k_z = 0$ (or in general two of the components are equal and the remaining is equal to zero) corresponds to the propagation of a wave along the unit cell face diagonal, the Γ - M direction in the first Brillouin zone, and the frequency dependence of the propagation constant component k_i now reads

$$k_{i1}^2 = \frac{1}{2} (k_0^2 - k_p^2) \quad i = x, y, z, \quad (19)$$

$$k_{i2}^2 = \frac{1}{4} \left[k_0^2 (l_0 + 1) - \sqrt{k_0^4 (l_0 - 1)^2 + 4k_0^2 k_p^2 l_0} \right] \quad i = x, y, z, \quad (20)$$

$$k_{i3}^2 = \frac{1}{4} \left[k_0^2 (l_0 + 1) + \sqrt{k_0^4 (l_0 - 1)^2 + 4k_0^2 k_p^2 l_0} \right] \quad i = x, y, z, \quad (21)$$

whereas solution (19) corresponds to a physical wave and is identical with (17), except for the value, and has the same frequency dependence. Solutions (20) and (21) do not correspond to any physical wave. In the case of $k_x = k_y = k_z$, the wave propagates along the unit cell diagonal, corresponding to the Γ - R direction in the first Brillouin zone. The physical solution of the frequency dependence

of the component $k_x = k_y = k_z$ is now

$$k_{i1}^2 = k_{i2}^2 = \frac{1}{18} [3k_0^2 (l_0 + 1) - k_p^2 - K_3] \quad i = x, y, z, \quad (22)$$

and the other two nonphysical solutions read

$$k_{i3}^2 = \frac{k_0^2 l_0 (k_p^2 - k_0^2)}{4k_p^2 - 3k_0^2} \quad i = x, y, z, \quad (23)$$

$$k_{i4}^2 = k_{i5}^2 = \frac{1}{18} [3k_0^2 (l_0 + 1) - k_p^2 + K_3] \quad i = x, y, z, \quad (24)$$

where

$$K_3 = \sqrt{9k_0^4 (l_0 - 1)^2 + 6k_0^2 k_p^2 (5l_0 - 1) + k_p^4}. \quad (25)$$

The real and imaginary parts of (22) are plotted in Fig. 4.

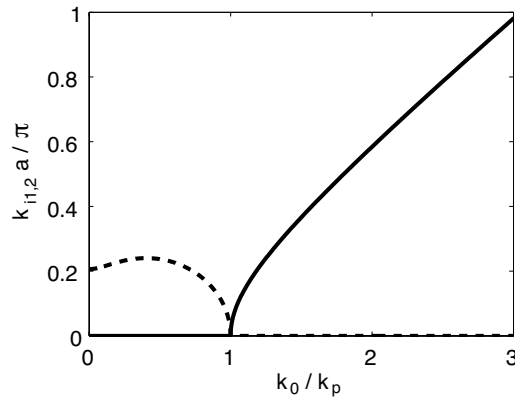


Figure 4. Frequency dependence of the propagation constant $k_{i1,2}$ ($i = x, y, z$) (22) both below and above the plasma frequency for the case that all of the propagation constant components are equal. The solid line corresponds to the real part, and the dashed line corresponds to the imaginary part, of the propagation constant.

The results presented above were obtained by solving Maxwell equations with a dielectric permittivity tensor in the form (1). It was shown, however, that the propagation constant solutions only suffer from weak spatial dispersion, moreover they are the same for the Γ - X and Γ - M directions and only the direction Γ - R differs. Thus we can assume that the medium is almost isotropic in the first Brillouin zone.

By substituting the simple isotropic model of permittivity in the form

$$\bar{\epsilon} = \left(1 - \frac{k_p^2}{k_0^2}\right) \bar{\mathbf{I}}. \tag{26}$$

into the eigenvalue Equation (10) we naturally obtain identical solutions for all of the important lattice directions, and they are equal to (17).

The comparison between the propagation constant predicted by the presented theory and the curves calculated by MWS is shown in Fig. 5. The propagation constant $k^2 = k_x^2 + k_y^2 + k_z^2$ now has one (Γ - X), two (Γ - M) or three (Γ - R) components and can be calculated as

$$k^2 = nk_i^2 \quad i = x, y, z, \quad n = 1, 2, 3, \tag{27}$$

where $n = 1$ and k_i is calculated with using (17) for the direction Γ - X , $n = 2$ and k_i is calculated with the use of (19) for the direction Γ - M and $n = 3$ and k_i is calculated with using (22). MWS calculates the dispersion characteristics of the wave propagating in the periodical medium [19]. Consequently, the curve calculated by MWS shows an upper stop band where no wave propagates. The boundary of this stop band is described by the condition of Bragg reflection $k_0a = \pi$. The presented theory uses a homogenized medium, therefore no such stop band can be seen and the propagation constant grows to infinity above the plasma frequency. Fig. 5 shows quite good agreement between

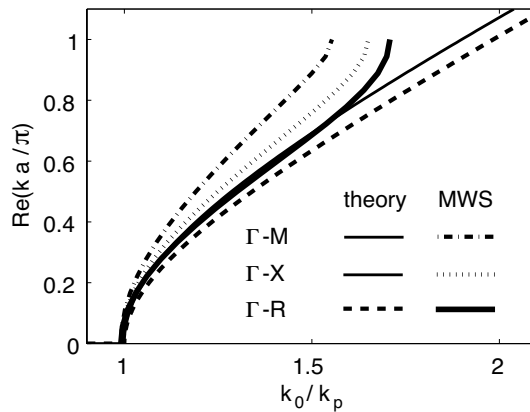


Figure 5. A comparison of the real part of the propagation constant $k^2 = k_x^2 + k_y^2 + k_z^2$ calculated by MWS and predicted by the presented theory for directions Γ - X , Γ - M and Γ - R .

the propagation constant predicted by the presented theory and the curves calculated by MWS in the close vicinity above the the plasma frequency. A difference can also be seen between the simulated curves for the Γ - X and Γ - M direction, which are the same, and the curve for the Γ - R direction. The propagation constant below the plasma frequency cannot be directly computed using MWS, but, the value of the phase constant calculated by the presented theory shows good agreement in the close vicinity below the plasma frequency, see Figs. 3 and 4.

4. NUMERICAL ANALYSIS

The triple wire medium was modeled by the CST Microwave Studio. The dispersion characteristics calculated by MWS are shown in Fig. 5. To verify the behavior of the wave in the lower stop band under the plasma frequency, the structure shown in Fig. 6 was analyzed. The structure forms one octant of the hollow sphere of triple wire material with the space period $a = 10$ mm. The inner sphere radius is 25 mm, and the outer radius is 105 mm. The wires are rectangular in cross section, with sides 0.85 mm in length. This shape simplifies the numerical simulation and at the same time shows the same plasma frequency $f_p = 9.28$ GHz as the wire medium composed of cylinders. The structure is fed by a dipole located at its center. Taking into

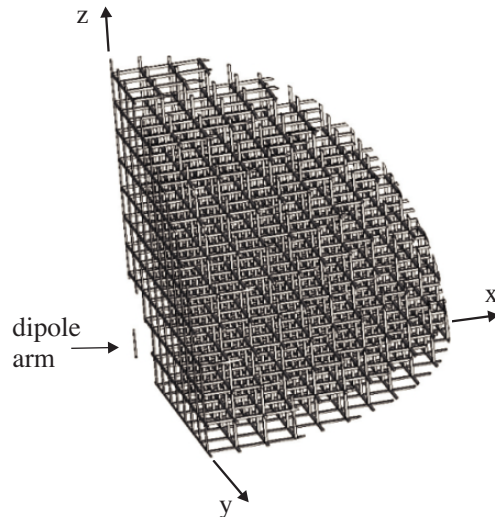


Figure 6. Analyzed 3D wire system.

account the excitation field symmetries, the octant is terminated at the x - y plane by a perfectly conducting wall and in the x - z and y - z planes by a perfectly magnetic wall. The field radiated by the dipole at frequencies below the plasma frequency is spread in the wire medium as evanescent waves with the distance dependence modified by the $1/r$ function [20]

$$|E| \approx E_0 \frac{e^{-\alpha r}}{r} \quad (28)$$

where α is the attenuation constant represented by the imaginary part of the propagation constant, and r is radial distance.

The electric field distribution calculated by MWS in the medium shown in Fig. 6 is plotted in Fig. 7 at frequency 7 GHz ($k_0/k_p \approx 0.75$). The calculated field represents the field in the microstructure, which is perturbed by the presence of the wires, as distinct from the averaged field, which defines the effective permittivity (1) [10]. However, the calculated field can be approximated by (28), as shown in Fig. 7. Similar plots have been obtained in the frequency band from 5 to 9 GHz. It may be noted from Fig. 7 that the field is attenuated at the same rate in all shown characteristic directions. This verifies the isotropy of the medium below the plasma frequency. Attenuation constant α can be estimated from the calculated field distributions, but does not fit well the data read from Figs. 3 and 4.

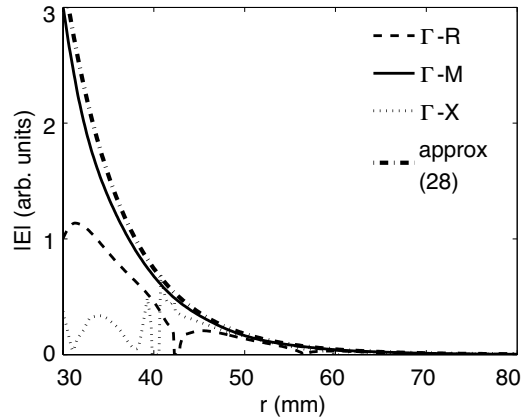


Figure 7. Distribution of the electric field in the medium from Fig. 6 at particular directions at frequency 7 GHz ($k_0/k_p \approx 0.75$). The line “approx” represents (28) with the value of α estimated as 120 m^{-1} .

5. CONCLUSION

This paper has studied the behavior of the triple wire medium with the aim to apply it as a negative permittivity isotropic metamaterial. The derivation of the dispersion equation of modes in the 3D lattice is quite straightforward, and the result is in accord with [10]. The numerical examples show that there exist eigen modes both below and above the plasma frequency in all important directions Γ - X , Γ - M and Γ - R , whereas we used two different models for the relative permittivity of the medium. Using only a simple isotropic model of permittivity (26), only physical solutions were found, and with the use of a more sophisticated model (1) both physical and nonphysical solutions were found. The physical modes comply with physical intuition, i.e., they are evanescent below the plasma frequency, and become propagating above the plasma frequency. Numerical simulations show that the other modes do not correspond to physical waves and this is the defect of the model (1). In the direction Γ - M , the attenuation and phase constants have the same amplitude as in the case of the direction Γ - X , since the propagation of the wave along one axis is equivalent to the propagation along the unit cell face.

From Fig. 2, it is obvious that the curves below (imaginary part) and above (real part) the plasma frequency form a circle, i.e., Equation (17) is an analytical expression of a circle. This implies isotropic propagation of the plane wave along one face of the triple wire cube. Since the structure is periodic, pass bands and stop bands should appear in the dispersion diagram. The curves calculated by MWS are in accord with this hypothesis, as it analyzes the structure as periodic, whereas the curves representing results of the presented theory are not. The reason is that we used a homogenized model of the triple wire medium. The triple wire medium behaves as an isotropic material for the wave propagating parallel with any coordinate plane. Taking into consideration the wave propagating in a general direction, the isotropy is now in general removed. However, a comparison of the dispersion characteristics calculated in various directions shows that in the first approximation the triple wire medium can be considered as an isotropic material in the close vicinity of the plasma frequency.

The modeling by the Microwave Studio verifies these theoretical results. The original numerical experiment shows the distribution of the electric field excited by the dipole located in the center of the sphere of the 3D wire material. The wave spreads in this system in the same way, except for the attenuation due to the negative permittivity, as in the empty space. The value of the attenuation constant and consequently the permittivity can be estimated from the resulting

distributions. The wave amplitude decreases at the same rate in all directions. This validates the isotropy of the medium even below the plasma frequency.

This paper proves that the triple medium of connected wires is a good candidate for an isotropic negative permittivity metamaterial.

ACKNOWLEDGMENT

This work has been supported in part by the Grant Agency of the Czech Republic under project 102/06/1106 "Metamaterials, nanostructures and their applications".

REFERENCES

1. Brown, J., "Artificial dielectrics," *Progress in Dielectr.*, Vol. 2, 193–225, 1960.
2. Rotman, W., "Plasma simulation by artificial dielectrics and parallel-plate media," *IRE Trans. Antennas Propag.*, Vol. 10, 82–84, 1962.
3. King, R., D. Thiel, and K. Park, "The synthesis of surface reactance using an artificial dielectric," *IEEE Trans. Antennas Propag.*, Vol. 31, Issue 3, 471–476, 1983.
4. Belov, P. A., S. A. Tretyakov, and A. J. Viitanen, "Dispersion and reflection properties of artificial media formed by regular lattices of ideally conducting wires," *Journal of Electrom. Waves and Applic.*, Vol. 16, No. 8, 1153–1170, 2002.
5. Nefedov, I. S. and A. J. Viitanen, "Guided waves in uniaxial wire medium slab," *Progress In Electromagnetics Research*, PIER 51, 167–185, 2005.
6. Pendry, J. B., A. J. Holden, W. J. Stewart, and I. Youngs, "Extremely low frequency plasmons in metallic mesostructures," *Phys. Rev. Lett.*, Vol. 76, 4773–4776, 1996.
7. Pendry, J. B., A. J. Holden, D. J. Robbins, and W. J. Stewart, "Low frequency plasmons in thin-wire structures," *J. Phys.: Condens. Matter*, Vol. 10, No. 22, 4785–4809, 1998.
8. Sievenpiper, D. F., M. E. Sickmiller, and E. Yablonovitch, "3D wire mesh photonic crystals," *Phys. Rev. Lett.*, Vol. 76, 2480–2483, 1996.
9. Belov, P. A., R. Marques, S. I. Maslovski, I. S. Nefedov, M. Silveirinha, C. R. Simovski, and S. A. Tretyakov, "Strong spatial dispersion in wire media in the very large wavelength limit," *Phys. Rev. B*, Vol. 67, 113103, 2003.

10. Silveirinha, M. G. and C. A. Fernandes, "Homogenization of 3-D-connected and nonconnected wire metamaterials," *IEEE Trans. Microwave Theory and Techn.*, Vol. 53, 1418–1430, 2005.
11. Simovski, C. R. and P. A. Belov, "Low-frequency spatial dispersion in wire media," *Phys. Rev. E*, Vol. 70, 0466161-1–8, 2004.
12. Nefedov, I. S., A. J. Viitanen, and S. A. Tretyakov, "Propagating and evanescent modes in two-dimensional wire media," *Phys. Rev. E*, Vol. 71, 046612-1–10, 2005.
13. Nefedov, I. S., X. Dardenne, C. Crayé, and S. A. Tretyakov, "Backward waves in a waveguide, filled with wire media," *Microwave and Opt. Techn. Lett.*, to be published.
14. Ikonen, P., M. Lapine, I. S. Nefedov, and S. A. Tretyakov, "Vector circuit theory for spatially dispersive uniaxial magneto-dielectric slabs," *Progress In Electromagnetics Research*, PIER 63, 279–294, 2006.
15. Dougherty, C., *Electrodynamics of Particles and Plasmas*, 175–178, Addison-Wesley, Reading, MA, 1969.
16. Shapiro, M. A., G. Shvets, J. R. Sirigiri, and R. J. Temkin, "Spatial dispersion in metamaterials with negative dielectric permittivity and its effect on surface waves," *Optics Express*, Vol. 31, 2051–2053, 2006.
17. Microwave Studio, Ver. 5.1, Computer Simulation Technology, Darmstadt, Germany, 2005.
18. Tretyakov, S. A., *Analytical Modeling in Applied Electromagnetics*, Artech House, Norwood, MA, 2003.
19. Smith, D. R., D. C. Vier, N. Kroll, and S. Schultz, "Direct calculation of permeability and permittivity for a left-handed metamaterial," *Applied Phys. Lett.*, Vol. 77, No. 14, 2246–2248, Oct. 2000.
20. Balanis, C. A., *Antenna Theory Analysis and Design*, John Wiley, New York, 1997.